

and from Eq. (7)

$$f_2(t_2) = -qt_2 + pa^2t_2/(b^2 + ct_2) \quad (11)$$

Substituting the corrected stress resultant $f_2(t_2)$ and its conjugate $\langle f_2(t_2) \rangle$ into the Eqs. (2) and (3), and evaluating the complex integrals the corresponding stress functions are determined as

$$\phi_{22}(z_2) = -pa^2b^2/c(cz_2 + b^2) \quad (12)$$

$$\psi_{22}(z_2) = pa^2/c - qb^2/z_2 - pa^2b^4/z_2(cz_2 + b^2) \quad (13)$$

Thus, the stress functions which are valid in the neighborhood of c_2 are expressed as the sum of the transformed stress functions and the adjusted ones, and they are

$$\phi_2(z_2) = \phi_{12}(z_1) + \phi_{22}(z_2) = -\frac{pa^2b^2}{c(cz_2 + b^2)} \quad (14)$$

$$\psi_2(z_2) = -pa^2/(z_2 + c) + pa^2/c - qb^2/z_2 - \frac{pa^2b^2}{c(cz_2 + b^2)}$$

The stress functions corresponding for the second approximation which is valid in the vicinity of c_1 can be obtained by a similar analysis starting from the hole c_2 , and they are

$$\phi_1(z_1) = -qa^2b^2/c(cz_1 - a^2)$$

$$\psi_1(z_1) = -qb^2/(z_1 - c) - pa^2/z_1 - qb^2/c - \frac{qa^2b^2}{c(cz_1 - a^2)} \quad (15)$$

The higher order approximations⁴ can be obtained by a similar process described above with no mathematical difficulties encountered. It can easily be shown that the successive approximation constructed in this manner converges, but the rapidity of convergence will depend on the magnitude of the parameters a, b, c, ϵ_1 , and ϵ_2 .

Numerical Results and Discussion

The numerical results for the distribution of stresses in the plate were obtained with the aid of digital computer for the case of $b = 2a$. In Fig. 1, the variation of the hoop stress along the line of symmetry is illustrated graphically for various spacing ($k = c/a$) of the holes. It shows that the high-stress concentrations always occur at the point F on c_1 and G on c_2 , and their magnitudes increase substantially as the holes get closer for the fixed radius ratio $b = 2a$. For instance, the stress at F is 4.75 times higher than that of the single inclusion for the case of $k = 3.1$ and $p = q$. As the spacing of the holes increases, the stress pattern rapidly converges to unity which is the exact result⁴ obtained in a single hole solution. Thus, for practice one can set a certain limit on the value of k beyond which the mutual effect of inclusions is not significant. The limit can be determined from Table 1, in which the maximum hoop stress at F is expressed in terms of p and q , by varying the radius ratio, ϵ_1 and ϵ_2 . It also shows that the maximum stress concentration at F is much more sensitive to the distances between the holes than moderate change in the radius ratio.

References

- ¹ Savin, G. N., *Stress Concentration Around Holes*, Pergamon Press, New York, 1961.
- ² Sokolinkoff, I. S., *Mathematical Theory of Elasticity*, 2nd ed., McGraw-Hill, New York, 1956, pp. 313-327.
- ³ Muskhelishvili, N. I., *Some Basic Problems of the Mathematical Theory of Elasticity*, Groninger-Holland, 1953, pp. 138-218.
- ⁴ Ukadgaonker, V. G., "Two Unequal Circular Inclusions in an Infinite Plate," M.S. thesis, 1970, Univ. of Rhode Island, Kingston, R. I.

Establishment Time of Laminar Separated Flows

MICHAEL S. HOLDEN

Cornell Aeronautical Laboratory Inc., Buffalo, N. Y.

I. Introduction

THE time required to establish steady flow in complex regions of viscous interaction and flow separation remains an important question despite over a decade of measurements in facilities with short run times such as shock tubes, shock tunnels, and piston and arc driven facilities. Measurements in shock tubes and shock tunnels at Cornell Aeronautical Laboratory (CAL) have indicated that separated regions can take from 100 μ sec to several msec to become fully established. Definitive measurements of the time establishment process in piston and arc driven facilities have in general not been possible because of the length and complexity of the starting process. For the set of measurements reported here a 40-ft driver section was fitted to the CAL 48 ft tunnel to give long test times at low incident Mach numbers. Figure 1 shows the test times available when the tunnel is operated under tailored interface conditions with 20- and 40-ft drivers. The boundary marking the appearance of the driver gas in the test section was determined from gas sampling techniques and heat transfer measurements ahead and in the base separated region. At incident shock Mach numbers of less than 2.5, we obtain running times greater than 20 msec.

II. Experimental Measurement

Base flow measurements

In the experimental studies of base flows, pressure and heat transfer measurements were made around spheres with diameters of 2, 6, 9, and 12 in., at Mach numbers from 6 to 8.5, unit Reynolds numbers from 2×10^6 to 9×10^6 , and T_w/T_∞ from 0.1 to 0.4. Typical pressure and heat transfer records ahead and in the base regions are shown in Fig. 2. For the conditions shown the nozzle flow and the attached boundary layers are fully established within 1.5 msec. The gross structure of the separated region is established first, with the pressure in the neighborhood of the separation point taking the longest time to stabilize; the fine structure, as indicated by the heat transfer close to the rear stagnation

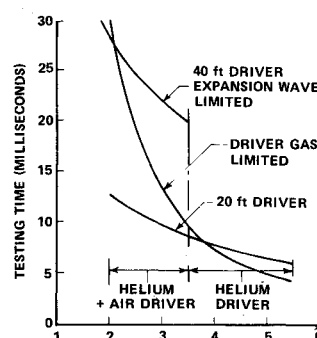


Fig. 1 Test time for tailored interface operation of 48 in. shock tunnel.

* Received April 22, 1971; revision received July 23, 1971. This experimental investigation was supported on CAL Feasibility Investigation Account 7152-442. Some measurements used in defining the time establishment of regions of shock wave-boundary layer interaction were taken in earlier experimental programs under Contracts AF 33(615)-1205 and F33615-67-C-1298 for the Air Force Aerospace Research Laboratories.

Index category: Nonsteady Aerodynamics.

* Principal Aerodynamicist, Aerodynamic Research Department. Associate Member AIAA.

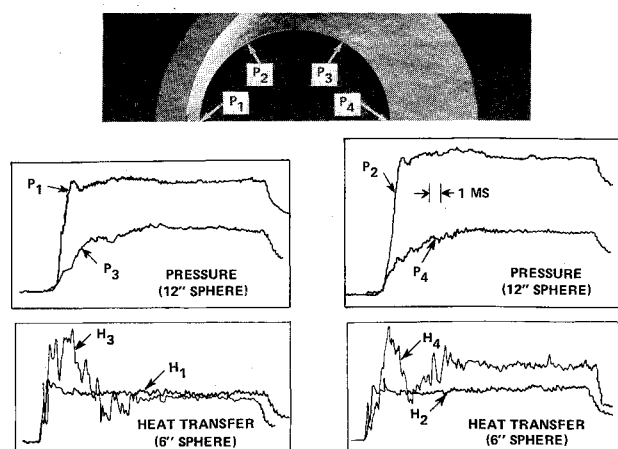


Fig. 2 Pressure and heat-transfer records during the establishment of a base separated flow.

point, takes longer to establish. The establishment processes measured in this study were an order of magnitude less than the running time of the tunnel, and the establishment times for pressure (τ_p) and heat transfer (τ_q) were defined when these quantities reached 98% of their final steady mean level.

Shock induced separation measurements

Detailed measurements of skin friction, pressure, and heat transfer made in regions of shock-wave-boundary-layer interaction gave us an opportunity to trace movement of the separation and reattachment points during flow establishment. These measurements were made on two-dimensional models both with and without side fences, over a wide range of freestream conditions. Figure 3 shows a series of skin friction, heat transfer, and pressure records obtained in a separated region at a flat plate-wedge junction. An examination of these records and many like them indicates that a small separated region is created during the starting process of the tunnel, this region growing in size during the steady running time to reach equilibrium approximately 2 msec after the start of steady airflows. Our measurements with a variety of spanwise configurations lead to the conclusion that the mechanism for the establishment of separated flow over these models is associated with establishment of flow in the streamwise plane perpendicular to the surface of the model rather than a phenomenon associated with establishment of lateral outflow or recirculation in a plane parallel to the surface of the model. The measurements indicate the leading edge of the separated region propagates forward with a speed close to that of the speed of sound at the wall.

III. Correlation of Time Establishment Measurements

The mechanism of flow establishment of separated base flow and regions of shock-wave-boundary-layer interaction is complex, and methods of estimating the establishment time based on mass, momentum, or energy entrainment using a steady-state model of the separated region are, in general, gross oversimplifications. The initial establishment mechanism is associated with the propagation of an acoustic or pressure disturbance from the controlling point in the flow-field—the neck or throat region in the base flow or the reattachment region in the shock-induced interaction region—to the forward extremity of the interaction region. The separated region then adjusts to reach equilibrium by viscous-inviscid interaction until conservation of momentum and energy are satisfied. In hypersonic flow these mechanisms take the same order of time. From similitude arguments we can express the characteristic establishment time test for

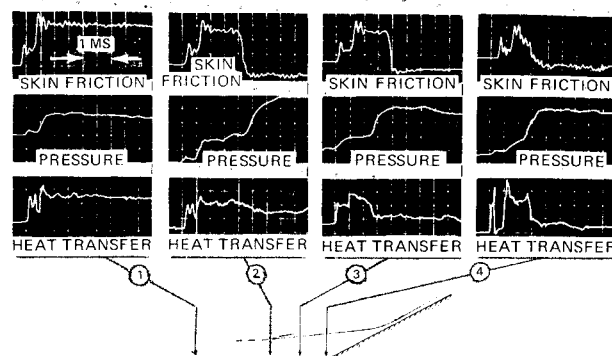


Fig. 3a Skin friction, pressures and heat-transfer records during the establishment of a base separated flow.

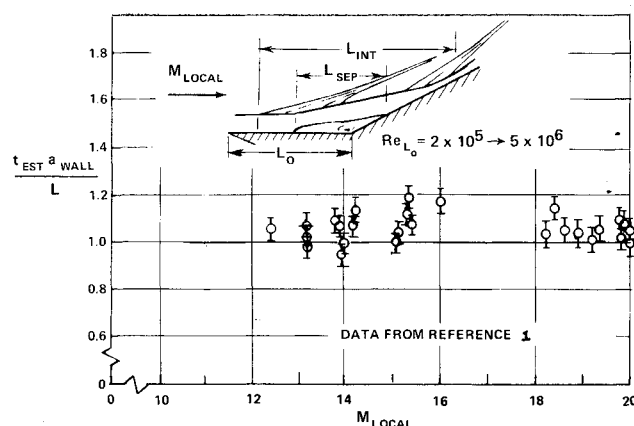


Fig. 3b Correlation of the establishment of shock-induced separated regions.

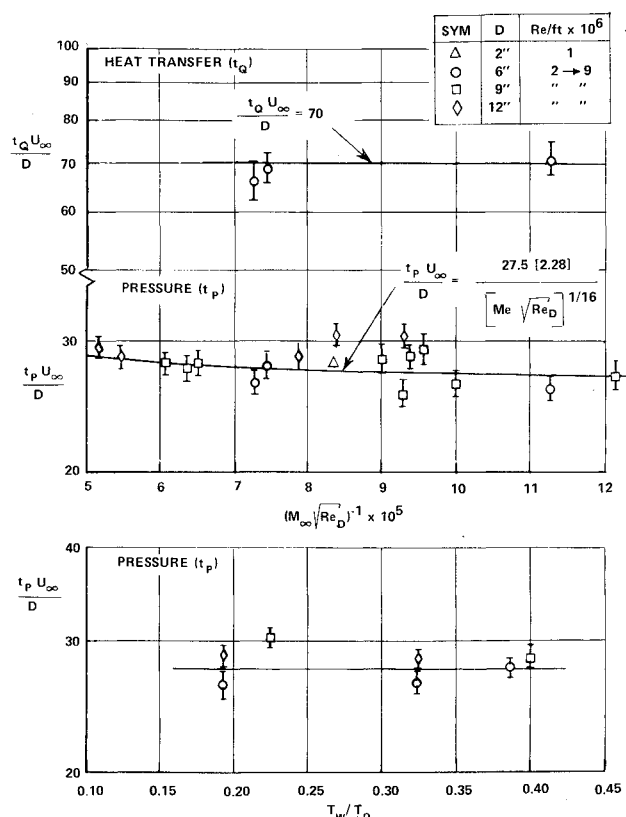


Fig. 4 Correlation of establishment of pressure and heat transfer in the base region of a sphere.

a given configuration in the form

$$(\tau_{\text{est}} \cdot U/L) = T(M_\infty, Re_L, T_w/T_\infty)$$

For the acoustic propagation the characteristic velocity U is the local speed of sound and L is a characteristic dimension related to the length of the interaction region through the parameter T_a . For the times to establish equilibrium of momentum and energy τ_p and τ_q , $T_{p,q}$ represents parameters which are related to the mixing process in the viscous shear layer and are significantly larger in fully laminar flows than in turbulent flows. Correlations of the measurements of the time required to achieve steady pressure and heat transfer levels in the base region behind the 4 spherical models over a range of freestream conditions are shown in Fig. 4. It can be seen that for the range of conditions studied the nondimensional establishment time is weakly influenced by the Mach number and Reynolds number of the freestream. The establishment time is directly proportional to the scale of the separated region and decreases with increasing freestream velocity. Because the establishment times we observe in these base flows are significantly longer than the acoustic time, we conclude that in these large separated regions the establishment of the viscous mixing is the dominant mechanism in attaining flow equilibrium. The heat transfer measurements, which take longer to stabilize, indicate that changes in the macroscopic structure of the base flow after the base pressure has stabilized do not significantly influence the gross properties of these regions. The measurements of the variation of base pressure with Reynolds number made in the present program together with earlier measurements made on spherical models, indicate the mixing process in the near wake was laminar in our studies.

The volumes of the separated regions which were studied in the work on shock-wave-boundary-layer interaction were very small in comparison to those encountered in the base flow studies and we found that the additional time required beyond the acoustic propagation time to attain flow equilibrium was small. Figure 3b shows a correlation of the measurements of time establishment nondimensionalized by the final interaction length and the acoustic propagation speed close to the wall. The experimental studies have shown that in these high temperature hypersonic flows the establishment times of separated regions depend strongly on size and geometry of the interaction regions. Whereas the time to establish the separated base flow behind a sphere is primarily dependent on the viscous mixing process to attain equilibrium, for the slender shock induced separated regions examined in our studies the establishment time can be found with good accuracy by calculating the time and pressure disturbances to traverse the entire length of the interaction region.

IV. Conclusions

Fitted with an extended driver section running times approaching 30 msec were obtained at low incident shock Mach numbers in the CAL 48 in. shock tunnel. Correlations of the measurements showed that just under 30 body lengths of flow ($t_p U/D = 27.9$) were required for the pressure in a base region to stabilize, with the heat transfer to this region taking a factor of two longer to reach equilibrium. The flow establishment time of a region of shock-wave-boundary-layer interaction could be found with good accuracy by calculating the time for an acoustic wave to traverse the total length of the interaction region, which in the present studies was less than 3 msec.

Reference

- Holden, M. S., "The Establishment Time of Laminar Separated Flows," Rept. 179, March 1971, Cornell Aeronautical Laboratory Inc., Buffalo, N.Y.

Thermodynamic Properties and Nozzle Flow of Hydrogen to 1000 atm and 100,000°K

R. W. PATCH*

NASA Lewis Research Center, Cleveland, Ohio

Introduction

THE need for reliable thermodynamic properties and nozzle-flow calculations for high-temperature hydrogen gas occurs in gaseous-core nuclear rockets and arcjets. A number of investigators have calculated high-temperature thermodynamic properties using a variety of assumptions. Rosenbaum and Levitt¹ included a covolume correction. McGee and Heller² included Debye-Hückel corrections. McChesney³ pointed out that McGee and Heller were inconsistent. Krascella⁴ used lowering of the ionization potential according to Ecker and Weizel,⁵ who later retracted their work.⁶ King⁷ assumed ideal gases in his thermodynamic property and nozzle flow calculations. Thus, previous to this author's work there were no reliable Debye-Hückel thermodynamic properties or nozzle flow calculations for hydrogen.

Thermodynamic Properties

The thermodynamic properties were based on compositions calculated by Patch.⁸ In Ref. 8 the species H , H^+ , e^- , H_2 , H^- , H_2^+ , and H_3^+ were included for conditions where each was important. Above 2000°K there was appreciable ionization, so the generally accepted Debye-Hückel approximation for charged particle interactions was used. Above 1300°K electronically excited states of H and H_2 were included, necessitating some sort of cutoff. For high degrees of ionization the perturbation of the energy levels is due principally to coulomb forces, so that one method of cutoff should be used, whereas for low degrees of ionization the perturbation of the energy levels is due principally to neutral particles, so that another method of cutoff should be used. Hence the cutoff was calculated by the Debye-Hückel method⁸ and a modified Bethe method,⁹ and the method which cut off the most states was used. It was assumed that the ortho-para ratios of the ground electronic states of H_2 and H_2^+ had their equilibrium values. For high degrees of ionization it was assumed the only species were H , H^+ , e^- , H^- , and H_2^+ , and equilibrium

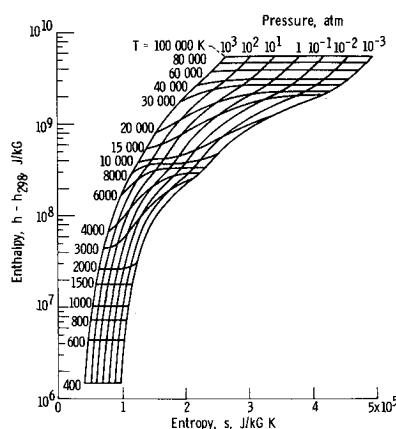


Fig. 1 Mollier diagram for hydrogen in chemical equilibrium in the Debye-Hückel approximation with equilibrium ortho-para ratio.

Received June 10, 1971.

* Research Scientist. Member AIAA.